

# Fundamental Physics using Gravitational Waves

NIUS Project Interim Report

Panchajanya Dey  
na2223-panchajanya  
[panchajanyad@iisc.ac.in](mailto:panchajanyad@iisc.ac.in)

January 2023

# Contents

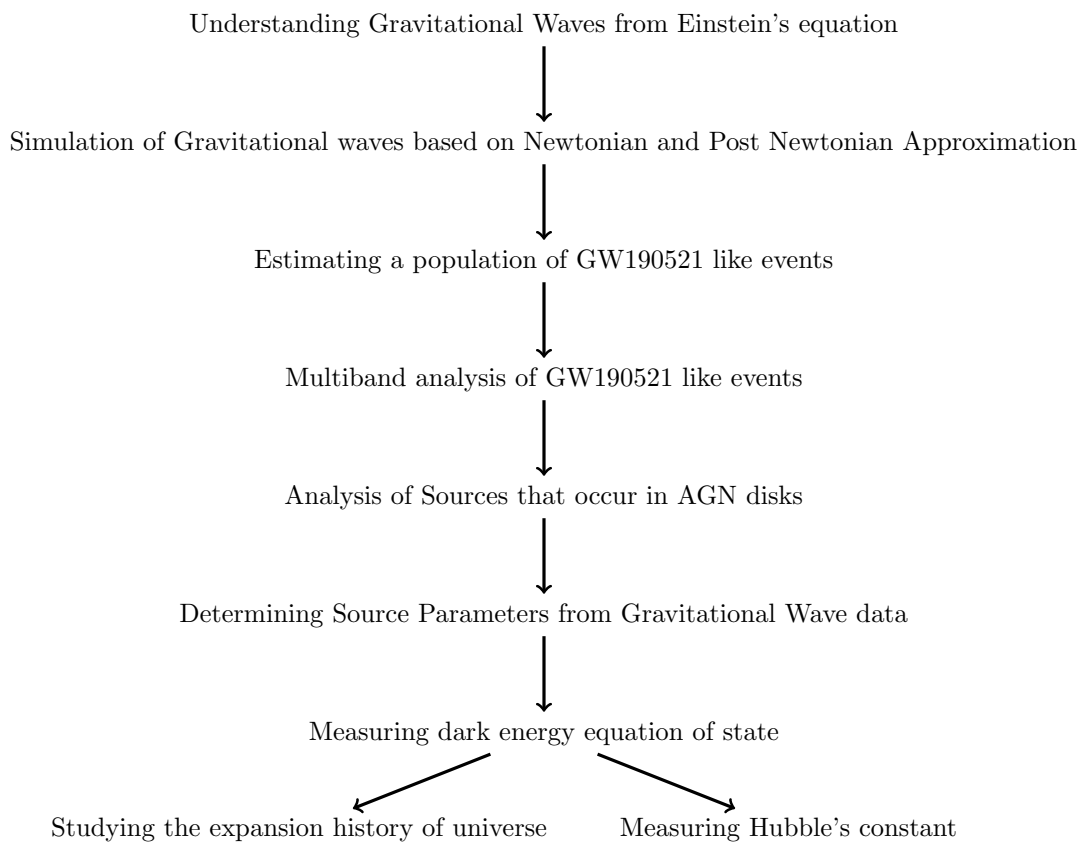
<b>1</b>	<b>Flow Chart for the Project</b>	<b>3</b>
<b>2</b>	<b>Introduction</b>	<b>4</b>
<b>3</b>	<b>Gravitational Waves in Linearized Theory</b>	<b>5</b>
3.1	Basics of Linearized Gravity . . . . .	5
3.2	Einstein Tensor in Linearized Gravity . . . . .	5
3.3	Einstein Field Equation in Linearized Gravity . . . . .	7
3.4	Properties of Gravitational Waves . . . . .	7
<b>4</b>	<b>Analysis of Binary System by Newtonian Approximation</b>	<b>8</b>
4.1	Introduction . . . . .	8
4.2	Equations with Explanations . . . . .	8
4.3	Simulation Results . . . . .	9
<b>5</b>	<b>Analysis of Binary System by Post-Newtonian Approximation</b>	<b>11</b>
5.1	Introduction . . . . .	11
5.2	Equations with Explanations . . . . .	11
5.3	Simulation Results . . . . .	12
<b>6</b>	<b>Analysis of GW190521 like Events</b>	<b>15</b>
6.1	Introduction . . . . .	15
6.2	Frequency Spectrum Analysis of GW190521 like Events . . . . .	15
6.2.1	Spectrum in LIGO Band . . . . .	15
6.2.2	Spectrum in LISA Band . . . . .	16
6.3	Estimation of GW190521 like events . . . . .	16
6.3.1	Constant merger rate model . . . . .	16
6.3.2	Delay Time Model . . . . .	17

# Abstract

This project aims to test Einstein's General Theory of Relativity from cosmological scales. This project also aims to estimate the composition of the universe over a significant period using luminosity distance  $d_l(z) = (1+z) \int_0^z \frac{cdz'}{H(z')}$ , which can be measured from the flux of the source. The sources used in this project are bright binary black hole(BBH) systems, i.e., BBHs that have an electromagnetic counterpart. This report includes what progress I have made during this project & the simulation of Gravitational waves using our codes.

# Chapter 1

## Flow Chart for the Project



**Milestone 1:** Understanding Gravitational Waves from Einstein's equation

**Milestone 2:** Simulation of Gravitational waves based on Newtonian and Post Newtonian Approximation

**Milestone 3 :** Developing GW tools for multi-band GW190521 analysis.

**Milestone 4 :** Testing General theory of relativity and the standard model of cosmology using multi-band observations.

## Chapter 2

# Introduction

In this project, we have studied the Gravitational-wave. The basic description of Gravitational wave and how it emerges from the Einstein equation is described in Chapter (3). For this purpose, we used the theory of linearised gravity to describe gravitational waves.

We have studied the Newtonian approximation for the generation of gravitational waves in the early inspiral phase of a binary black hole system. Then we simulated the gravitational wave signal for a binary black hole system when the separation between the component black holes is large enough that the orbital speed of the black holes is non-relativistic so that Newtonian approximation holds. These are described in Chapter (4).

The next Chapter (5) describes the generation of Gravitational waves from a binary Black hole system till the late inspiral phase using the post-Newtonian approximation. We have used the results of the 2PN approximation. Then we simulated the gravitational wave signal for a binary black hole system using our code. We can see the *Chirp* behavior of the gravitational wave signal from a binary black hole merger.

In Chapter (??), we analyze the Gravitational-wave signal obtained from a GW190521-like event and also estimate the number of such events till a certain redshift within a period of one year. We used the constant merger rate model and the delay time model separately to estimate the number of such events.

Studying Gravitational waves to understand our universe is an up-and-coming and recently explored field. The difficulties of detecting Gravitational waves from distant sources were the main problem, as gravitation is the weakest of all fundamental forces. But, development in this field over the last few decades has opened the door to studying gravitational waves from distant binary mergers and, therefore, studying the history of the universe's composition.

There are three types of compact binary systems, binary Neutron Stars(BNSs), Neutron Star Black Hole Binary and, binary Black Holes(BBHs). Of them, the strength of Gravitational wave signals is maximum for the BBHs and minimum for BNSs. Therefore, BBHs can be detected in high redshifts as high as  $z = 1$ , where BNSs can be detected till redshifts of  $z = 0.1$ . therefore, studying BBHs allows us to look back in time.

## Chapter 3

# Gravitational Waves in Linearized Theory

### 3.1 Basics of Linearized Gravity

As a reference, I followed Flanagan and Hughes 2005[4] and Schutz and Ricci 1999[6] for studying this topic. Linearized gravity is an adequate approximation technique in which the space-time metric  $g_{\mu\nu}$  deviates from the flat space-time metric  $\eta_{\mu\nu}$  only by a slight margin  $h_{\mu\nu}$ . The flat space-time metric  $\eta_{\mu\nu}$  is defined as a diagonal matrix, with the sign  $(-, +, +, +)$ , i.e.,  $\eta_{\mu\nu} = \text{diag}(-1, 1, 1, 1)$ . Then the space-time metric  $g_{\mu\nu}$  can be written as:

$$g_{\mu\nu} = \eta_{\mu\nu} + h_{\mu\nu} \text{ where, } \| h_{\mu\nu} \| \ll 1. \quad (3.1)$$

Since,  $\eta_{\mu\nu}$  describes the flat space-time metric in a cartesian coordinate system, imposing the condition  $\| h_{\mu\nu} \| \ll 1$  requires both the gravitational field to be weak and also the coordinate system to be approximately cartesian. In linearized theory, the smallness of  $h_{\mu\nu}$  allows us to neglect any term of the order  $O(h^2)$  or higher. Therefore, indices are raised using  $g^{\mu\nu}$ , which is given as:

$$g^{\mu\nu} = \eta^{\mu\nu} - h^{\mu\nu} \quad (3.2)$$

### 3.2 Einstein Tensor in Linearized Gravity

The Einstein tensor  $G_{\mu\nu}$  is defined as:

$$G_{\mu\nu} = R_{\mu\nu} - \frac{1}{2}g_{\mu\nu}R \quad (3.3)$$

where the Ricci Tensor  $R_{\mu\nu}$  can be obtained by contracting the Riemann Tensor  $R^\alpha_{\beta\gamma\delta}$ , and the Ricci scalar  $R$  is obtained by contracting the Ricci Tensor. The Riemann Tensor is defined as:

$$R^\alpha_{\beta\gamma\delta} = \partial_\gamma \Gamma^\alpha_{\beta\delta} - \partial_\delta \Gamma^\alpha_{\beta\gamma} \quad (3.4)$$

where,  $\Gamma^\alpha_{\beta\gamma}$  is the Christoffel coefficient given by,

$$\Gamma^\lambda_{\mu\nu} = \frac{1}{2}g^{\lambda\alpha}(\partial_\mu g_{\alpha\nu} + \partial_\nu g_{\alpha\mu} - \partial_\alpha g_{\mu\nu}) = \frac{1}{2}g^{\lambda\alpha}(\partial_\mu h_{\alpha\nu} + \partial_\nu h_{\alpha\mu} - \partial_\alpha h_{\mu\nu}) = \frac{1}{2}(\partial_\mu h^\lambda_\nu + \partial_\nu h^\lambda_\mu - \partial^\alpha h_{\mu\nu}) \quad (3.5)$$

which is accurate to the order  $O(h^2)$

$$\begin{aligned} \text{Now, } R^\alpha_{\beta\gamma\delta} &= \partial_\gamma \Gamma^\alpha_{\beta\delta} - \partial_\delta \Gamma^\alpha_{\beta\gamma} \\ &= \frac{1}{2}(\partial_\gamma [\partial_\beta h^\alpha_\delta + \partial_\delta h^\alpha_\beta - \partial^\alpha_{\beta\delta}] - \partial_\delta [\partial_\beta h^\alpha_\gamma + \partial_\gamma h^\alpha_\beta - \partial^\alpha_{\beta\gamma}]) \\ &= \frac{1}{2}(\partial_\gamma \partial_\beta h^\alpha_\delta + \partial_\delta \partial^\alpha h_{\beta\gamma} - \partial_\gamma \partial^\alpha h_{\beta\delta} - \partial_\delta \partial_\beta h^\alpha_\gamma) \end{aligned}$$

Contracting the Riemann Tensor  $R_{\beta\gamma\delta}^\alpha$  by taking  $\alpha = \gamma$  we have,  
 $R_{\beta\delta} = R_{\beta\gamma\delta}^\gamma = \frac{1}{2}(\partial_\gamma\partial_\beta h_\delta^\gamma + \partial_\delta\partial^\gamma h_{\beta\gamma} - \partial_\gamma\partial^\gamma h_{\beta\delta} - \partial_\delta\partial_\beta h_\gamma^\gamma)$

Now,  $\partial_\gamma\partial^\gamma$  is the d'Alembert operator and  $h_\gamma^\gamma$  is the trace of  $h_\beta^\alpha$  which we will denote by  $h$ .  
 So,

$$R_{\beta\delta} = \frac{1}{2}(\partial_\gamma\partial_\beta h_\delta^\gamma + \partial_\delta\partial^\gamma h_{\beta\gamma} - \square h_{\beta\delta} - \partial_\beta\partial_\delta h) \quad (3.6)$$

Now, we have the Ricci Tensor, we can find the Ricci Scalar by contracting once more. For that,  $R_\beta^\alpha = g^{\alpha\delta}R_{\beta\delta} = \eta^{\alpha\delta}R_{\beta\delta}$ , accurate to the order of  $O(h^2)$   
 So,  $R_\beta^\alpha = \frac{1}{2}(\partial_\gamma\partial^\alpha h_\beta^\gamma + \partial_\beta\partial^\gamma h_\gamma^\alpha - \square h_\beta^\alpha - \partial^\alpha\partial_\beta h)$

Then,  $R = R_\beta^\beta$   
 $= \frac{1}{2}(\partial_\gamma\partial^\beta h_\beta^\gamma + \partial_\beta\partial^\gamma h_\gamma^\beta - \square h_\beta^\beta - \partial^\beta\partial_\beta h)$   
 $= (\partial_\gamma\partial^\beta h_\beta^\gamma - \square h)$   
 So,

$$R = \partial_\gamma\partial^\beta h_\beta^\gamma - \square h \quad (3.7)$$

Now, the Einstein Tensor  $G_{\mu\nu}$  can be constructed on the basis of (3.6) and (3.7).

$$\begin{aligned} G_{\alpha\beta} &= R_{\alpha\beta} - \frac{1}{2}g_{\alpha\beta}R \\ &= R_{\alpha\beta} - \frac{1}{2}\eta_{\alpha\beta}R \\ &= \frac{1}{2}(\partial_\gamma\partial_\alpha h_\beta^\gamma + \partial_\beta\partial^\gamma h_{\alpha\gamma} - \square h_{\alpha\beta} - \partial_\alpha\partial_\beta h) - \frac{1}{2}\eta_{\alpha\beta}(\partial_\gamma\partial^\delta h_\delta^\gamma - \square h) \end{aligned}$$

So,

$$G_{\alpha\beta} = \frac{1}{2}(\partial_\gamma\partial_\alpha h_\beta^\gamma + \partial_\beta\partial^\gamma h_{\alpha\gamma} - \square h_{\alpha\beta} - \partial_\alpha\partial_\beta h - \eta_{\alpha\beta}\partial_\gamma\partial^\delta h_\delta^\gamma + \eta_{\alpha\beta}\square h) \quad (3.8)$$

This expression can be simplified to an extent by a change in the notation, where instead of using the metric perturbation, we use the trace-reversed perturbation:

$$\bar{h}_{\alpha\beta} = h_{\alpha\beta} - \frac{1}{2}\eta_{\alpha\beta}h \quad (3.9)$$

In this notation,  $\bar{h}_\alpha^\gamma = \eta^{\gamma\beta}\bar{h}_{\alpha\beta}$   
 $= h_\alpha^\gamma - \frac{1}{2}\delta_\alpha^\gamma h$

So,  $\bar{h} = \bar{h}_\alpha^\alpha = h_\alpha^\alpha - \frac{1}{2}\delta_\alpha^\alpha h$   
 $= h - \frac{1}{2} \times 4h = h - 2h = -h$

That's why it is called the trace-reversed transformation.

Applying Trace-Reversed transformation on (3.8), all terms with the trace  $h$  are canceled and the transformed equation becomes:

$$G_{\alpha\beta} = \frac{1}{2}(\partial_\gamma\partial_\beta \bar{h}_\alpha^\gamma + \partial^\gamma\partial_\alpha \bar{h}_{\beta\gamma} - \square \bar{h}_{\alpha\beta} - \eta_{\alpha\beta}\partial_\gamma\partial^\delta \bar{h}_\delta^\gamma) \quad (3.10)$$

This equation can be further simplified by using coordinate transformation which is known as *Gauge Transformation*. Define a coordinate frame  $x^{\alpha'} = x^\alpha + \xi^\alpha$ . This transformation changes the metric such that:

$$h'_{\alpha\beta} = h_{\alpha\beta} - \partial_\alpha\xi_\beta - \partial_\beta\xi_\alpha \quad (3.11)$$

This is obtained because:

$$\begin{aligned} g_{\alpha\beta} &= \frac{\partial x^{\gamma'}}{\partial x^\alpha} \frac{\partial x^{\delta'}}{\partial x^\beta} g'_{\gamma\delta} \\ &= g'_{\gamma\delta} + \partial_\gamma\xi_\delta + \partial_\delta\xi_\gamma \end{aligned}$$

Which gives the equation (3.11).

If Einstein's General Relativity is valid on a large scale then any metric perturbation can be put into a Lorentz Gauge by making an infinitesimal coordinate transformation as mentioned above. Applying the Lorentz Gauge transformation on (3.10), a simplified equation arises:

$$G_{\alpha\beta} = -\frac{1}{2}\square\bar{h}_{\alpha\beta} \quad (3.12)$$

### 3.3 Einstein Field Equation in Linearized Gravity

The Einstein Field Equation connects the geometry of space-time to the distribution of matter within it by:

$$G_{\alpha\beta} = \frac{8\pi G}{c^4}T_{\alpha\beta} \quad (3.13)$$

In a vacuum,  $T_{\alpha\beta} = 0$ , so the vacuum Einstein Field Equation in Linearized Gravity becomes:

$$\square\bar{h}_{\alpha\beta} = 0 \quad (3.14)$$

The d'Alembert operator is basically  $(\frac{1}{c^2}\frac{\partial^2}{\partial t^2} - \nabla^2)$ , so the equation (3.14) admits a class of homogenous solution which are the superposition of plane waves all propagating with a speed of  $c$ . This is how gravitational waves arise in linearized gravity.

### 3.4 Properties of Gravitational Waves

The linearized theory describes a classical gravitational field which can be described as a massless spin 2 field that propagates at the speed of light. Such a field has only two independent degrees of freedom, called polarization in classical terms. A gravitational wave described by (3.14) has two polarizations called plus and cross polarizations denoted by  $h_+$  and  $h_\times$ , respectively. Gravitational waves are mainly dominated by quadropolar moment, unlike electromagnetic waves, which are dominated by the dipolar moment of the source producing it.



## Chapter 4

# Analysis of Binary System by Newtonian Approximation

### 4.1 Introduction

For this analysis, I have referred Cutler and Flanagan 1994 [3] and Antelis et al. 2018 [2]. The Newtonian approximation is used to describe two compact objects rotating around a common center of mass and slowly approaching each other by emitting energy in the form of gravitational waves. This description of a compact binary is accurate only when the orbital velocity of both objects is much lower than the speed of light. This implies that Newtonian Approximation will only hold when the orbiting objects are far enough from each other so their orbital velocity is much less than the speed of light. The early phase of the inspiral can be modeled accurately by Newtonian approximation, where the Newtonian quadrupole formula describes the gravitational wave.

### 4.2 Equations with Explanations

For a binary system comprising two masses  $M_1$  and  $M_2$ , with orbital separation  $r$ , let, total mass =  $M = M_1 + M_2$ , reduced mass =  $\mu = \frac{M_1 M_2}{M}$ , and, chirp mass =  $\mathcal{M} = \mu^{3/5} M^{2/5}$ . The orbital frequency  $\Omega$  is given by (Assuming  $G = 1$ , and,  $c = 1$ ):

$$\Omega = \frac{M^{1/2}}{r^{3/2}} \quad (4.1)$$

Assuming the orbit to be circular, the inspiral rate is given by,

$$\frac{dr}{dt} = -\frac{r}{E} \frac{dE}{dt} = -\frac{64}{5} \frac{\mu M^2}{r^3} \quad (4.2)$$

Assuming point masses, the collision occurs when the orbital separation  $r = 0$ , we denote this time by  $t_c$ . Integrating (4.2) till  $t_c$  we have,

$$r = \left(\frac{256}{5} \mu M^2\right)^{1/4} (t_c - t)^{1/4} \quad (4.3)$$

Since the emitted gravitational waves are quadrupolar, the angular frequency of the gravitational wave =  $2\Omega$ , i.e., the frequency is  $\Omega/\pi$ . The gravitational waves can be quantified by the strain produced by it at the detector denoted by  $h(t)$ . The strain is given as:

$$h(t) = \frac{(384/5)^{1/2} \pi^{2/3} Q(\theta, \varphi, \psi, \iota) \mu M}{Dr(t)} \cos\left(\int 2\pi f dt\right) \quad (4.4)$$

Here,  $D$  is the distance to the source, and  $Q$  is a function determined by the position and orientation of the binary source. The change in frequency with time is given by:

$$\frac{df}{dt} = \frac{96}{5} \pi^{8/3} \mathcal{M}^{5/3} f^{11/3} \quad (4.5)$$

Note that all these formulae are valid only when the separation  $r$  is much large. The experimental frequency can be obtained from the Fourier Transform of strain vs. time data, and then it can be used to determine the parameters of the binary. The phase of the waveform can be found by:

$$\phi(t) = \int_{-\infty}^t 2\pi f(t') dt' \quad (4.6)$$

The gravitational wave has two transverse polarization modes: plus and cross polarisation. The strain produced by them is given by:

$$h_+(t) = A \frac{1 + \cos^2 \iota}{2} \cos(2\pi f_{gw} t_{ret} + 2\phi) \quad (4.7)$$

$$h_{\times}(t) = A \cos \iota \sin(2\pi f_{gw} t_{ret} + 2\phi) \quad (4.8)$$

Where,  $t_{ret}$  corresponds to the retarded time defined as  $t_{ret} = t - \frac{1}{c}|x - x'|$ , that accounts for the finite speed of propagation of Gravitational Waves from source to an observer.  $A$  is the amplitude, and  $\iota$  is the inclination angle of the source.  $\phi$  is the phase of the wave. The frequency of the gravitational wave  $f_{gw}$  is given by:

$$f_{gw}(t) = \frac{c^3}{8\pi GM} (\Theta(t))^{-3/8} \quad (4.9)$$

And the phase is:

$$\phi(t) = -\frac{2c^3}{5GM} (\Theta(t))^{-3/8} (t_c - t) + \phi_c \quad (4.10)$$

The parameter  $\Theta(t)$  in equation (4.9) and (4.10) is defined by:

$$\Theta(t) := \frac{\nu c^3}{5GM} (t_c - t) \quad (4.11)$$

A gravitational wave detector actually detects a combination of the plus polarisation strain and the cross polarisation strain, which depends on the orientation of the detector. The strain detected by the detector is given by:

$$h(t) = F_+ h_+(t) + F_{\times} h_{\times}(t) \quad (4.12)$$

Where,  $F_+$  and  $F_{\times}$  are the antenna parameters given in terms of Euler angles  $\theta$ ,  $\varphi$  and  $\psi$  by:

$$F_+ = -\frac{1}{2}(1 + \cos^2 \theta) \cos 2\varphi \cos 2\psi - \cos \theta \cos 2\varphi \sin 2\psi \quad (4.13)$$

$$F_{\times} = \frac{1}{2}(1 + \cos^2 \theta) \cos 2\varphi \sin 2\psi - \cos \theta \sin 2\varphi \cos 2\psi \quad (4.14)$$

### 4.3 Simulation Results

Based on the previous section (4.2), the following graph for strain vs time is obtained when  $t \ll t_c$  so that Newtonian Approximation holds. All the codes used in this section to run the simulations are completely developed by us and we have not taken the reference of any already existing code.

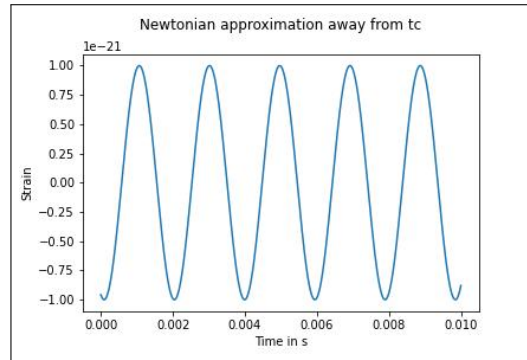


Figure 4.1: Strain Vs Time for  $t \ll t_c$  in Newtonian Approximation

Though the frequency appears to be constant in the figure, it is actually increasing with time, but for such large separation between the objects, the frequency is apparently constant. The amplitude is also increasing but the rate of increment is too small to be seen in the graph.

## Chapter 5

# Analysis of Binary System by Post-Newtonian Approximation

### 5.1 Introduction

In the previous chapter (4), we have seen that Newtonian approximation can model the early inspiral phase of the binary quite accurately but fails in the late inspiral phase. Therefore, post-Newtonian approximations are used to model the late inspiral phase. There are many orders of post-Newtonian approximations depending on the level of accuracy needed in a problem. In our analysis, we shall be using the post-Newtonian approximation of order 2, i.e., 2PN approximations. For this analysis, I have referred Antelis et al. 2018 [2]. Post-Newtonian approximation accurately describes the inspiral phase, but numerical relativity models are required for the merger and ringdown phase.

### 5.2 Equations with Explanations

In 2PN approximation, the phase  $\phi_{gw}(t)$  is given by:

$$\phi_{gw}(t) = \phi_0 - \frac{1}{\eta} \left( \Theta(t)^{5/8} + \left( \frac{3715}{8064} + \frac{55}{96}\eta \right) \Theta(t)^{3/8} - \frac{3\pi}{4} \Theta(t)^{1/4} + \left( \frac{9275495}{14450688} + \frac{284875}{258048}\eta + \frac{1855}{2048}\eta^2 \right) \Theta(t)^{1/8} \right) \quad (5.1)$$

And, the frequency  $f_{gw}$  is given by:

$$f_{gw}(t) = \frac{c^3}{8GM} \left( \Theta(t)^{-3/8} + \left( \frac{743}{2688} + \frac{11}{32}\eta \right) \Theta(t)^{-5/8} - \frac{3\pi}{10} \Theta(t)^{-3/4} + \left( \frac{1855099}{14450688} + \frac{56975}{258048}\eta + \frac{371}{2048}\eta^2 \right) \Theta(t)^{-7/8} \right) \quad (5.2)$$

Here,  $\eta$  is the symmetric mass ratio defined as  $\eta = \frac{M_1 M_2}{M^2}$ ,  $\Theta(t)$  is same as (4.11).

In this case, the gravitational wave induces a strain  $h(t)$  given by:

$$h(t) = \frac{A(t)}{D} \cos(2\phi_{gw}(t) - \theta) \quad (5.3)$$

Here,  $A(t)$  is the time-dependent quadrupolar amplitude given by the equation:

$$A(t) = -\frac{2G\mu}{c^4} (\pi G M f_{gw}(t))^{2/3} \quad (5.4)$$

$\theta$  is a phase angle comprising the antenna parameters and inclination angle, such that  $\tan \theta = \frac{F_{\times}}{F_{+}} \frac{2 \cos \iota}{1 + \cos^2 \iota}$ . If  $r$  is the proper distance of the source, then,  $\mathcal{D}$  is the effective distance of the source given by:

$$\mathcal{D} = \frac{r}{\sqrt{F_{+}^2 \left( \frac{1 + \cos^2 \iota}{2} \right)^2 + F_{\times}^2 \cos^2 \iota}} \quad (5.5)$$

So, the effective distance is in general greater than the real distance  $r$ . Only when the source is optimally oriented, we have,  $\mathcal{D} = r$ .

### 5.3 Simulation Results

The following graph is a plot between Strain vs time data for a binary black hole system with each of its component mass =  $50M_{\odot}$ . The start time is 200 ms before the time of coalescence( $t_c$ ). It is clear from the graph that in the late inspiral phase, the frequency of gravitational wave increase rapidly, as well as the amplitude. This gives rise to the chirping behavior of the gravitational wave signal from a binary black-hole merger. We completely developed all the codes used in this section to run the simulations, and we have not taken the reference of any already existing code.

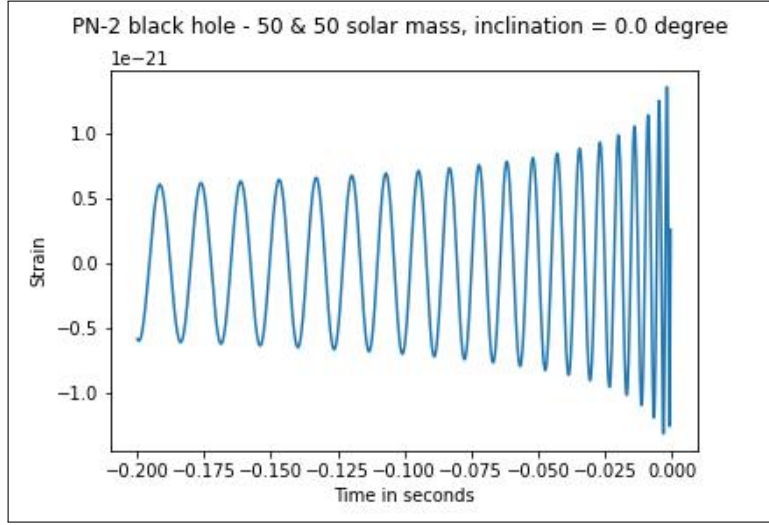


Figure 5.1: Strain vs time for 2PN approximation

The graph below describes the Amplitude ( $A(t)$ ) of the gravitational wave as a function of half of the total mass of the binary system, where we have taken primary mass = secondary mass =  $\frac{totalmass}{2}$  for simplicity. The amplitude is measured keeping the frequency of the Gravitational Wave( $f_{gw}$ ) constant.

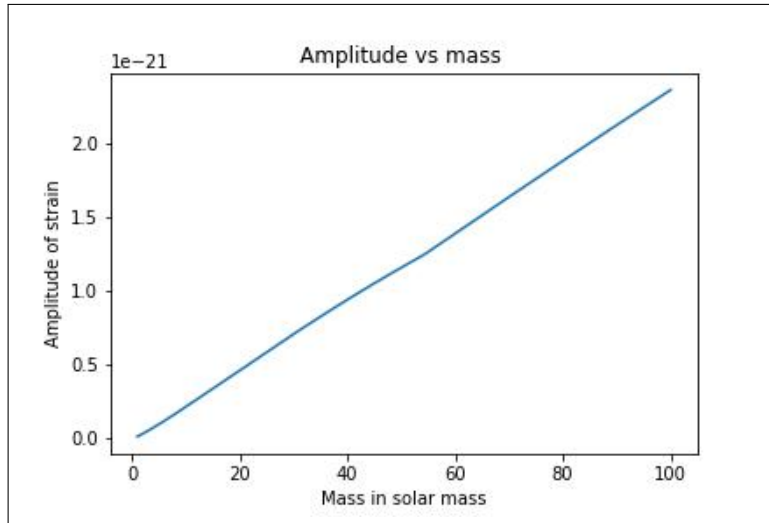


Figure 5.2: Amplitude vs half of Total Mass for 2PN approximation

The graph indicates that amplitude is proportional to the total mass of the binary.

The graph below describes the amplitude of the  $l=2, m=2$  Gravitational wave signal vs mass of one component of the binary, keeping the total mass of the binary system fixed at  $100M_{\odot}$ .

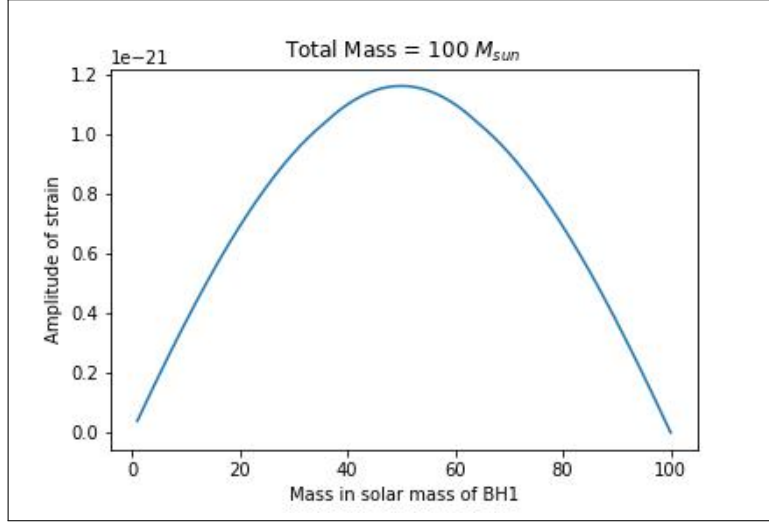


Figure 5.3: Amplitude vs Component Mass for 2PN approximation keeping total mass fixed

Clearly, the  $l=2, m=2$  Gravitational wave signal peaks when the mass ratio is 1.

The following figure describes the maximum frequency of the Gravitational Wave vs the component mass where we assumed primary mass = secondary mass for simplicity.

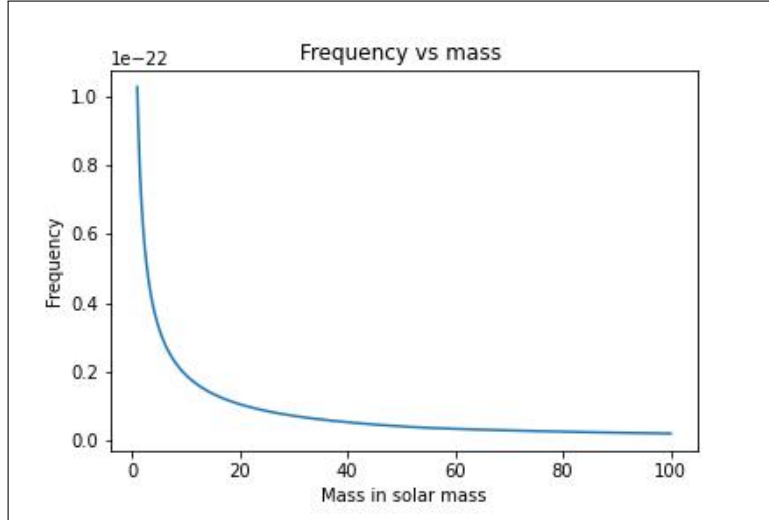


Figure 5.4: Frequency vs Component Mass for 2PN approximation

As the graph suggests, the maximum frequency decreases with an increase in the component mass. This can be described by the separation of the black holes at the time of coalescence. The separation of their centers is proportional to the sum of the radius of the black holes. And for black-hole, the Schwarzschild radius is given as  $R = \frac{2GM}{c^2}$ , so a more massive black hole has a larger radius. So, if the binary consists of larger component masses, then during coalescence, the separation between component masses would be more, and as frequency is approximately proportional to  $\frac{M^{1/2}}{r^{3/2}}$ , we can say  $f \propto 1/M$ .

The following figure describes the dependence of strain on the inclination angle.

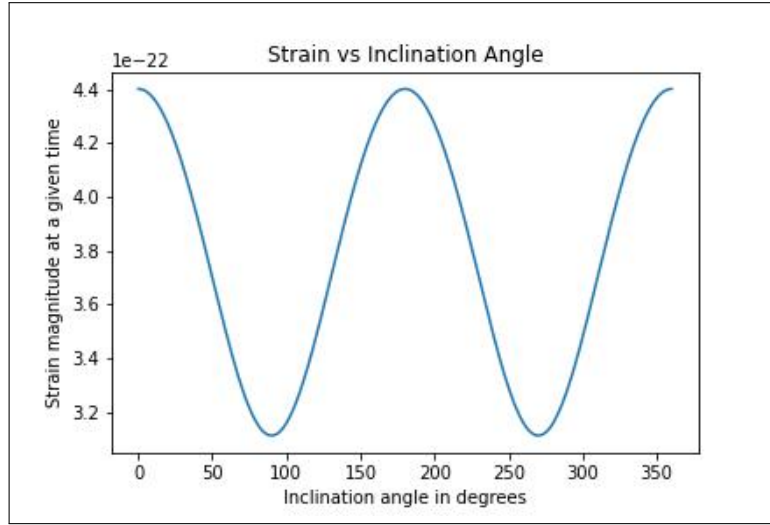


Figure 5.5: Strain vs Inclination angle for 2PN approximation

The strain is maximum when the angular momentum of the binary points directly at the detector or point directly opposite to the detector. And it is minimum when it points in a direction which is perpendicular to the line joining the detector and the source.

## Chapter 6

# Analysis of GW190521 like Events

### 6.1 Introduction

For this section, I have studied from R. Abbott et al.[1]. GW190521 is a short-duration gravitational-wave signal detected on May 21, 2019, at 03:02:29 UTC by LIGO Hanford, LIGO Livingston, and Virgo observatories. Post-detection modifications and analysis indicated that GW190521 could be from a quasicircular binary inspiral, and it is consistent with the merger of a binary black-hole system with primary mass  $85M_{\odot}$  and secondary mass  $66M_{\odot}$ . The mass of the final black hole =  $142M_{\odot}$ . The estimated redshift of the event is 0.82. This is a bright binary source i.e., an electromagnetic counterpart is associated with it.

### 6.2 Frequency Spectrum Analysis of GW190521 like Events

For this part, we first generated the strain vs time data for a binary Black Hole with the parameters same as GW190521. Then, the obtained data is Fourier Transformed to obtain the Frequency Spectrum of the event. The frequency spectrum is obtained individually in two bands, the LIGO Band: 10 Hz to 10 kHz, and, the LISA Band: 0.1 mHz to 1 Hz. We completely developed all the codes used in this section to run the simulations, and we have not taken the reference of any already existing code. The LIGO band analysis is done by Adith and I have done the LISA band analysis.

#### 6.2.1 Spectrum in LIGO Band

The following graph shows the spectrum of a GW190521-like event in the LIGO band.

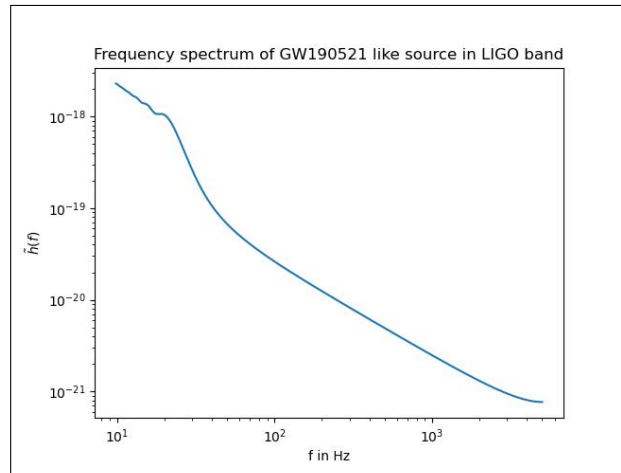


Figure 6.1: Spectrum of a GW190521 like event in LIGO band



### 6.2.2 Spectrum in LISA Band

The following graph shows the spectrum of a GW190521-like event in the LISA band.

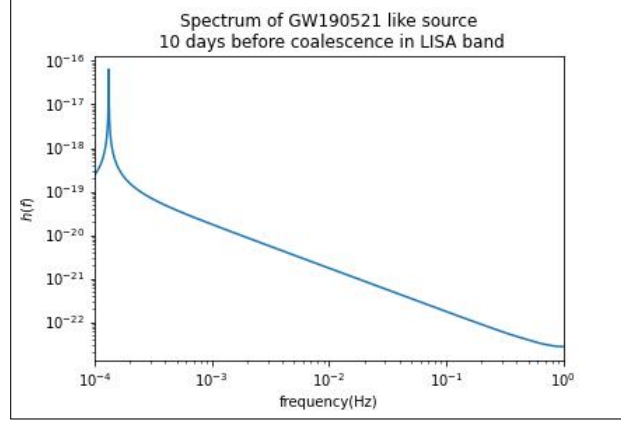


Figure 6.2: Spectrum of a GW190521 like event in LISA band

## 6.3 Estimation of GW190521 like events

In this section, the number of GW190521-like events till a redshift for a period of one year is estimated using two different models. For reference, I followed arxiv.2210.05724[5]. The constant merger rate model considers a single parameter  $R_0$ , which corresponds to a scenario with no redshift evolution. The delay time model r is a physics-driven model that models the merger rate in terms of the delay time distribution denoted by  $t_d$ .

### 6.3.1 Constant merger rate model

Here, we have taken the parameter  $R_0$  to be equal to  $0.13 \text{ Gpc}^{-3} \text{ yr}^{-1}$  which is the infrared rate of mergers similar to GW190521. Now, the number of such events per unit redshift per unit time is given by:

$$\frac{dN_{gw}}{dt dz} = \frac{R(z)}{1+z} \frac{dV_c}{dz}(\theta_c) \quad (6.1)$$

Where,  $\theta_c$  is the set of cosmological parameters and, for constant merger model  $R(z) = R_0$ . The graph of the number of such events over one year till a redshift limit is attached below.

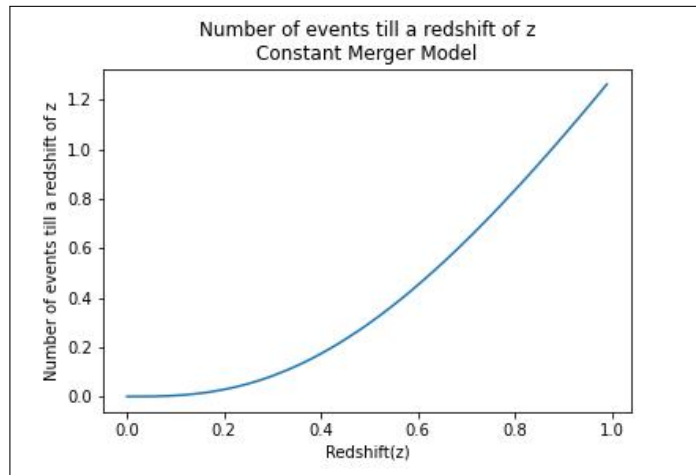


Figure 6.3: Number of events till a redshift of z in constant merger model

### 6.3.2 Delay Time Model

In this case,  $R(z)$  is defined as:

$$R(z) = R_0(1+z)^\gamma \frac{1 + (1+z_p)^{-(\gamma+\kappa)}}{1 + \left(\frac{1+z}{1+z_p}\right)^{\gamma+\kappa}} \quad (6.2)$$

The parameters are given as:  $\gamma = 2.7, \kappa = 2.9, z_p = 1.9$ .

For finding  $R_0$ , we have to consider that  $R(z = 0.82) = 0.13 \text{ Gpc}^{-3}\text{yr}^{-1}$ . This gives,  $R_0 = 0.028 \text{ Gpc}^{-3}\text{yr}^{-1}$ .

The graph of the number of such events over one year till a redshift limit is attached below. We completely developed all the codes used in this section to run this simulation, and we have not taken the reference of any already existing code.

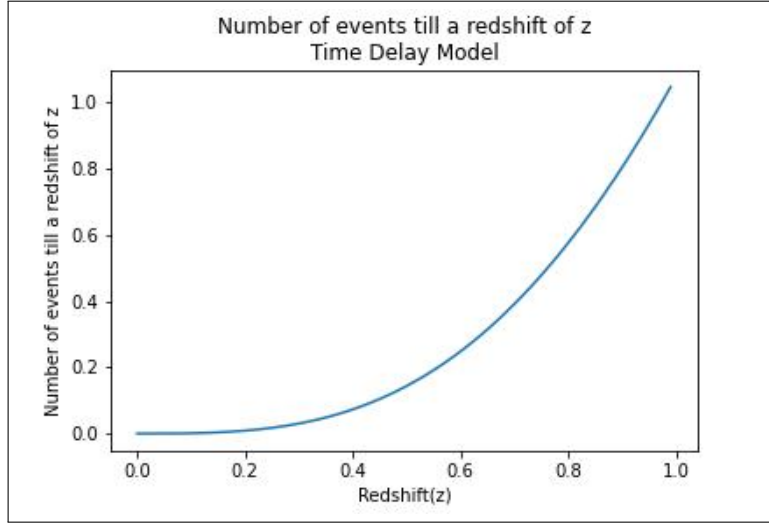


Figure 6.4: Number of events till a redshift of  $z$  in time delay model

## Acknowledgement

The work in this report was done with my partner Adith Praveen of IIT Madras, under the supervision of Prof(Dr). Suvodip Mukherjee, TIFR, Colaba, Mumbai. This project work is implemented in python using the libraries NumPy, Matplotlib, and SciPy. No other external code has been used in the work mentioned in this report. **We acknowledge the support of our mentor Dr. Suvodip Mukherjee and the NIUS program of HBCSE-TIFR funded by the Department of Atomic Energy, Govt. of India (Project No. RTI4001).**

# Bibliography

- [1] R. Abbott et al. “GW190521: A Binary Black Hole Merger with a Total Mass of  $150M_{\odot}$ ”. In: *Physical Review Letters* 125.10 (Sept. 2020). DOI: [10.1103/physrevlett.125.101102](https://doi.org/10.1103/physrevlett.125.101102). URL: <https://doi.org/10.1103%2Fphysrevlett.125.101102>.
- [2] Javier M. Antelis, Jaime M. Hernández, and Claudia Moreno. “Post-Newtonian approximation of gravitational waves from the inspiral phase”. In: *Journal of Physics: Conference Series* 1030.1 (May 2018), p. 012005. DOI: [10.1088/1742-6596/1030/1/012005](https://dx.doi.org/10.1088/1742-6596/1030/1/012005). URL: <https://dx.doi.org/10.1088/1742-6596/1030/1/012005>.
- [3] Curt Cutler and Éanna E. Flanagan. “Gravitational waves from merging compact binaries: How accurately can one extract the binary’s parameters from the inspiral waveform?”. In: *Physical Review D* 49.6 (Mar. 1994), pp. 2658–2697. DOI: [10.1103/physrevd.49.2658](https://doi.org/10.1103/physrevd.49.2658). URL: <https://doi.org/10.1103%2Fphysrevd.49.2658>.
- [4] Éanna É Flanagan and Scott A Hughes. “The basics of gravitational wave theory”. In: *New Journal of Physics* 7 (Sept. 2005), pp. 204–204. DOI: [10.1088/1367-2630/7/1/204](https://doi.org/10.1088/1367-2630/7/1/204). URL: <https://doi.org/10.1088%2F1367-2630%2F7%2F1%2F204>.
- [5] Christos Karathanasis et al. *GWSim: A python package to create GW mock samples for different astrophysical populations and cosmological models of binary black holes*. 2022. DOI: [10.48550/ARXIV.2210.05724](https://arxiv.org/abs/2210.05724). URL: <https://arxiv.org/abs/2210.05724>.
- [6] Bernard F Schutz and Franco Ricci. “Gravitational Waves, Sources, and Detectors”. In: (2010). DOI: [10.48550/ARXIV.1005.4735](https://arxiv.org/abs/1005.4735). URL: <https://arxiv.org/abs/1005.4735>.